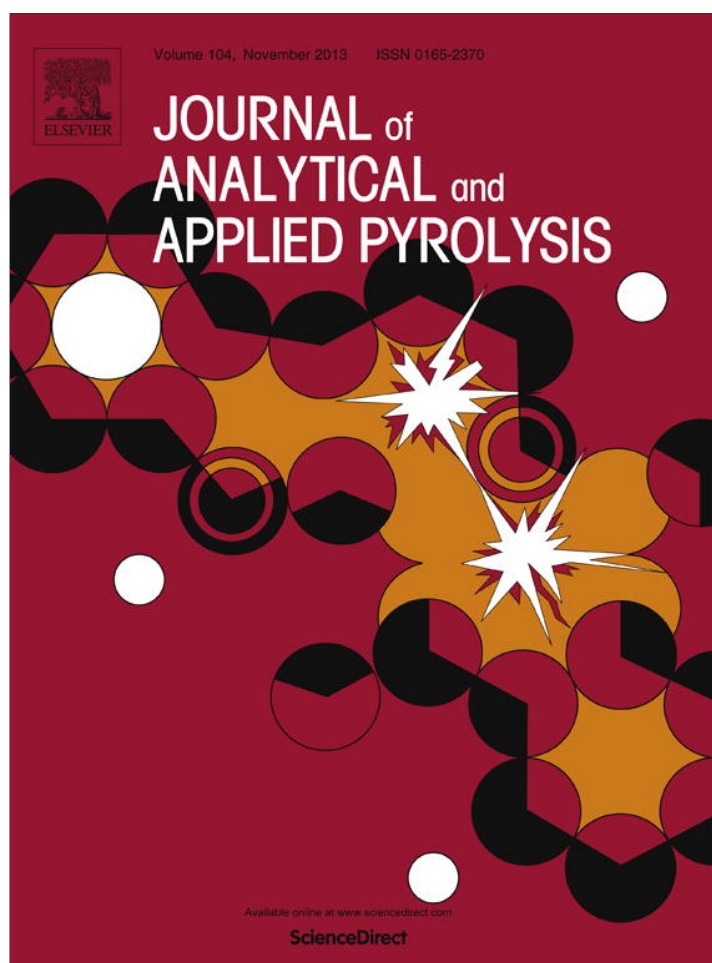


Provided for non-commercial research and education use.
Not for reproduction, distribution or commercial use.



This article appeared in a journal published by Elsevier. The attached copy is furnished to the author for internal non-commercial research and education use, including for instruction at the authors institution and sharing with colleagues.

Other uses, including reproduction and distribution, or selling or licensing copies, or posting to personal, institutional or third party websites are prohibited.

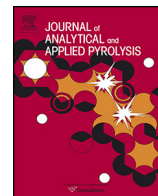
In most cases authors are permitted to post their version of the article (e.g. in Word or Tex form) to their personal website or institutional repository. Authors requiring further information regarding Elsevier's archiving and manuscript policies are encouraged to visit:

<http://www.elsevier.com/authorsrights>



Contents lists available at ScienceDirect

Journal of Analytical and Applied Pyrolysis

journal homepage: www.elsevier.com/locate/jaap

Thermal stability of some cryogels based on poly(vinyl alcohol) and cellulose



Cristian-Drăgăș Varganici^a, Oana Maria Paduraru^a, Liliana Rosu^a, Dan Rosu^{a,*},
Bogdan C. Simionescu^{a,b}

^a Centre of Advanced Research in Bionanoconjugates and Biopolymers, "Petru Poni" Institute of Macromolecular Chemistry, 41A Gr. Ghica-Voda Alley, 700487 Iasi, Romania

^b Department of Natural and Synthetic Polymers, "Gh. Asachi" Technical University of Iasi, 73 Dimitrie Mangeron Boulevard, 700050 Iasi, Romania

ARTICLE INFO

Article history:

Received 26 April 2013

Accepted 6 September 2013

Available online 16 September 2013

Keywords:

Cryogels

Thermogravimetric analysis

Thermal decomposition kinetics

Evolved gas analysis

ABSTRACT

The aim of this study consisted in the elucidation of the thermal decomposition process of some cellulose and poly(vinyl alcohol) based cryogels as films. The thermal behavior was studied by dynamic thermogravimetry and differential scanning calorimetry in nitrogen atmosphere, up to 600 °C. Evolved gases analysis were performed using a coupling to a quadrupole mass spectrometer and a Fourier transform infrared spectrophotometer equipped with external modulus for gas analyses. Global kinetic parameters of the thermal decomposition process were determined by applying the isoconversional differential method of Friedman and the integral method of Flynn–Wall–Ozawa. The final form of the kinetic model and the parameters for each individual stage of thermal decomposition were determined by multivariate non-linear regression method.

© 2013 Elsevier B.V. All rights reserved.

1. Introduction

Cellulose, the most abundant natural polymer on the planet, possesses the capacity to easily engage in intermolecular interactions with other polymers or polymer based systems. Interactions of cellulose with synthetic polymers are mainly based on hydrogen bonding established between hydroxyl groups of the glucose ring and functional groups of the polymers [1]. Cellulose based materials present some disadvantages, such as limited solubility in organic solvents. Such materials are hydrophilic, polar and manifest strong interactions between polar groups. These properties harden the dispersion of cellulose in the melted state of the synthetic polymer thus leading to low adhesion between cellulose and the polymer scaffold [2]. Surpassing these difficulties can be achieved through the following procedures: (i) using of a coupling agent [3,4]; (ii) chemical modification of cellulose, in order to allow the obtaining of films, followed by a regeneration stage [5]; (iii) solubilizing the cellulose in an adequate solvent and re-precipitation followed by the obtaining of fibers or films [6]. Reported literature studies refer to some systems based on unmodified cellulose (fiber, viscose, powder) and synthetic polymers or blends based on different cellulose derivatives [7].

Poly(vinyl alcohol) (PVA) is a water-soluble, non-toxic, biodegradable, biocompatible synthetic polymer with excellent

film forming properties. Due to its large number of hydroxyl groups, PVA exhibits a strong hydrophilic and hydrogen bonding character, thus being able to form crosslinked hydrogels. Its high polarity and water solubility makes PVA suitable for the obtaining of blends with natural polymers. Cryogels based on PVA and polysaccharides may be applied for wound dressing due to their biocompatibility, flexibility, good mechanical strength and barrier agents against microorganisms [8].

In this paper authors report the investigations on the thermal decomposition process of cellulose and PVA based cryogels with the purpose of gaining new knowledge on their thermal stability in inert atmosphere as background to industrial processing of the future material with biomedical applications.

2. Experimental

2.1. Materials

PVA with an average molecular weight of 146,000–186,000 and a hydrolysis degree of 99% was purchased from Aldrich. Microcrystalline cellulose Avicell PH-101 was purchased from Fluka.

2.2. Synthesis

Cryogels with PVA as scaffold and increasing cellulose content were synthesized following a procedure described in a previous paper [8]. According to the procedure a PVA solution of 8 wt% concentration was prepared by dissolving of a certain amount of PVA in

* Corresponding author. Tel.: +40 232 217 45; fax: +40 232 211 299.
E-mail addresses: dan.rosu50@yahoo.com, drosu@icmpp.ro (D. Rosu).

Table 1
Cryogels composition.

Sample	Code	Cryogels composition	
		PVA (%)	Cellulose (%)
PVA	PVA	100	0
90/10	P1	90	10
70/30	P3	70	30
50/50	P5	50	50
Cel	Cel	0	100

double distilled water at a temperature of 90 °C and under stirring for a time of 8 h. A clear solution was obtained. Varying quantities of microcrystalline cellulose were dispersed in 11/1 water/NaOH (w/w) mixture, stirred for 5 min and afterwards frozen at low temperature (−30 °C). After defrosting, the obtained solutions were stirred and clear transparent solutions were obtained [9]. Cellulose and PVA solutions were mixed in different ratios (Table 1) and afterwards stirred for 5 min. The mixtures were poured on Petri dishes and frozen at −20 °C for 12 h, and after that thawed at room temperature (25 °C) for another 12 h. The freezing/thawing process was repeated three times. The blank PVA cryogel was prepared by pouring a certain amount of PVA solution on a Petri dish and then exposed to three freezing/thawing cycles (12 h freezing/12 h thawing). The PVA and the PVA/cellulose cryogels were washed for 3 days with distilled water and then they were dried by lyophilization for 24 h, using a LABCONCO 117 freezing-dryer. Polymeric films were obtained after lyophilization. Since the cellulose cryogel could not be obtained by this technique, the cellulose powder was used as blank sample after it was first treated in the same conditions as described above.

2.3. Measurements

The thermal degradation and evolved gas analyses were performed with a TGA–FTIR–MS system. The system was equipped with an apparatus of simultaneous TGA/DSC analyses STA 449F1 Jupiter model (Netzsch, Germany), FTIR spectrophotometer Vertex-70 model (Bruker, Germany) and a mass spectrometer QMS 403C Aeolos model (Netzsch, Germany). The TG/DSC thermobalance was coupled online with FTIR spectrophotometer and mass spectrometer through two heated transfer lines. 9 mg of each sample was heated from 30 to 600 °C under nitrogen flow (flow rate 50 mL min^{−1}), in an open Al₂O₃ crucible and Al₂O₃ as reference material was used. Heating rates of 5, 10, 20 and 40 °C min^{−1} were applied. The transfer line to FTIR spectrophotometer was made of polytetrafluorethylene, had an interior diameter of 1.5 mm and was heated at 290 °C. The spectra were acquired with a spectral resolution of 4 cm^{−1} on 400–4000 cm^{−1} range. The transfer line to MS spectrometer QMS 403C is made of a quartz capillary with an internal diameter of 75 μm and was heated at 290 °C. The mass spectra were recorded under electron ionization energy of 70 eV. Data were scanned in the range *m/z* = 1–300, the measuring time for each cycle was 150 s. The NIST Mass Spectral Database was used for the identification of ion fragments (*m/z*) in MS spectra. The kinetic analysis of thermogravimetric data was performed using the soft Netzsch Thermokinetic 3.

3. Results and discussion

3.1. Thermal stability

Thermal stability comparative studies between the cryogels and the pure comprising polymers were published elsewhere [8]. It was reported that the pure cellulose decomposed in two stages of thermal decomposition, exhibiting a major thermal degradation

stage in the second step at a temperature lower than 300 °C with a maximum temperature peak at 345 °C. The pure PVA and cryogels decomposed in four stages, according to the first derivative curves (DTGs) peaks. For pure PVA, the initial decomposition temperature value of stage three, where the highest degree of mass loss occurred, was at 306 °C. Although the initial decomposition temperature values of the first two stages of the cryogels presented shifts to lower temperature domains with increasing cellulose content, these values became intermediate to the ones corresponding to the pure components beginning with stage three of thermal decomposition. The residual mass depended on the cellulose content and the DTG curves peaks for the second stage of thermal degradation of the cryogels decreased in intensity. These aspects clearly demonstrate the occurrence of hydrogen bonding between the two pure components, thus leading to an enhancement of the cryogels thermal stabilities. The hydrogen bonding occurs between hydroxyl groups of the glucose ring and hydroxyl groups of the PVA. The simultaneous TG/DTG/DSC thermograms for cryogel coded P5 are presented in Fig. 1. The TG and DTG thermograms clearly show the four thermal decomposition stages, thus being in good agreement with the reported literature [8]. The DSC curves exhibited four endothermic processes characteristic to each individual thermal decomposition stage. The other cryogels exhibited similar thermal behaviors.

3.2. Thermal decomposition kinetics

It was assumed that the thermal decomposition process of the studied films is described by the reaction model given in Eq. (1), where the solid material M(s) decomposes into solid residue A(s) and gases B(g).



The kinetic parameters were evaluated from non-isothermal experiments. The conversion degree (α) was calculated using Eq. (2), where m_i , m_t and m_f represent the weights of the sample before degradation, at a time t , and after complete degradation.

$$\alpha = \frac{m_i - m_t}{m_i - m_f} \quad (2)$$

The conversion rate is described by Eq. (3), where t is time (min), A is the pre-exponential factor (s^{−1}), E is the activation energy of thermal decomposition (kJ mol^{−1}), R is the gas constant (8.314 J K^{−1} mol^{−1}), T is temperature (K) and $f(\alpha)$ is the conversion function.

$$\frac{d\alpha}{dt} = Ae^{-E/RT}f(\alpha) \quad (3)$$

A new equation of the thermal degradation rate is obtained by inserting the rate of heating (Eq. (4)), $\beta = dT/dt$.

$$\frac{d\alpha}{dT} = \frac{A}{\beta} e^{-E/RT}f(\alpha) \quad (4)$$

Global kinetic parameters were evaluated by applying two isoconversional methods which use shifts in thermograms with heating rate increase, due to temperature delay as a function of heating rate [10–12].

The method proposed by Friedman [13] uses the differential form of the rate equation (Eq. (5)):

$$\ln \frac{d\alpha}{dt} = \ln \beta \frac{d\alpha}{dT} = \ln[Af(\alpha)] - \frac{E}{RT} \quad (5)$$

The plot of $\ln d\alpha/dt$ versus $1/T$, for $\alpha = \text{const}$ extracted from the thermograms recorded at different heating rates should be a straight line whose slope allows an evaluation of the activation energy [13].

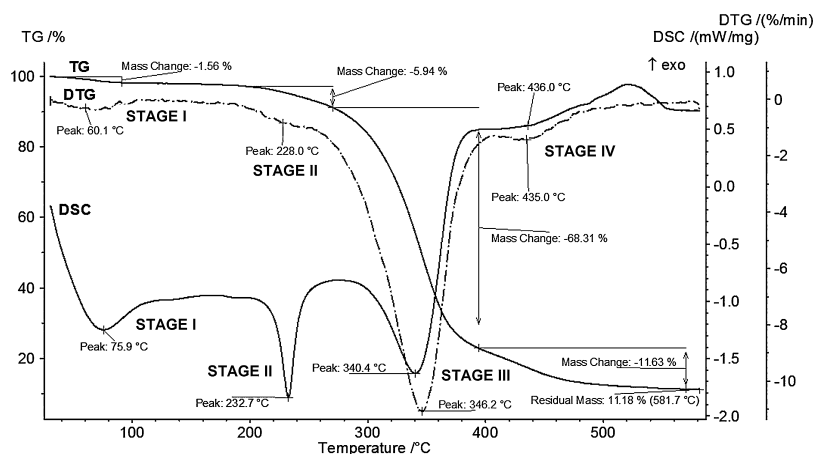


Fig. 1. TG, DTG and DSC thermograms for sample P5.

After integration of Eq. (4) between the limits T_0 and T_p the integral function of conversion was obtained and was noted $G(\alpha)$ in Eq. (6).

$$G(\alpha) = \frac{A}{\beta} \int_{T_0}^{T_p} e^{-E/RT} dT = \int_0^{\alpha_p} \frac{d\alpha}{f(\alpha)} \quad (6)$$

T_0 is the initial temperature corresponding to $\alpha=0$ and T_p is the temperature corresponding to the peak from DTG curve, where $\alpha=\alpha_p$. The integral function of conversion depicts the mechanism of thermal degradation [14].

The second applied method is the integral one of Flynn–Wall–Ozawa [15–17] which uses the Doyle approximation [18] of the temperature integral in Eq. (6). The relationship between kinetic parameters and the heating rate is given by Eq. (7).

$$\ln \beta = \ln \left(\frac{AE}{R} \right) - \ln G(\alpha) - 5.3305 - 1.052 \frac{E}{RT} \quad (7)$$

To calculate the kinetic parameters with Eq. (7), it was considered that the process was described by a first order reaction for $G(\alpha)$. For the same value of α , the plot of $\ln \beta$ as a function of $1/T$ is a straight line with the slope proportional with the activation energy.

The non-isothermal data extracted from the thermograms were processed with the software Netzsch Thermokinetics 3. As an exemplification, the sample P5 was taken into account, due to the similar thermal behavior exhibited by the other cryogels. Figs. 2 and 3 show the graphics of the Friedman and Flynn–Wall–Ozawa plots respectively, at α values ranging between 0.1 and 0.9, for the sample P5. The thermal decomposition in four successive stages is confirmed by the slope of the straight lines variation in Fig. 2. The straight lines from Fig. 3 are not parallel, thus the assumption of a first order reaction model for $f(\alpha)$ function is not the best option. Both isoconversional methods indicate the dependence of the activation energy on the conversion degree. The values of the global kinetic parameters obtained through the two applied isoconversional methods for sample P5 are given in Table 2. The differences between kinetic parameters calculated by the two methods were explained in the literature [19,20].

It can be observed from Table 2 that in all four stages of thermal decomposition the values of the kinetic parameters increase with the conversion degree, suggesting a complex decomposition mechanism through successive and/or parallel reactions [21]. The possibility to apply a kinetic model of independent parallel reactions, as those commonly applied to natural polymeric materials, such as biomass [22,23], was first taken into account. However, an inadequate correlation between the experimental and simulated data was obtained in this case. Furthermore, this study was

conducted for pure cellulose based cryogels and in inert atmosphere. These aspects may yield significant differences between thermal decomposition mechanisms of biomass in oxidative atmospheres and the discussed hydrogels in inert atmosphere. Due to the

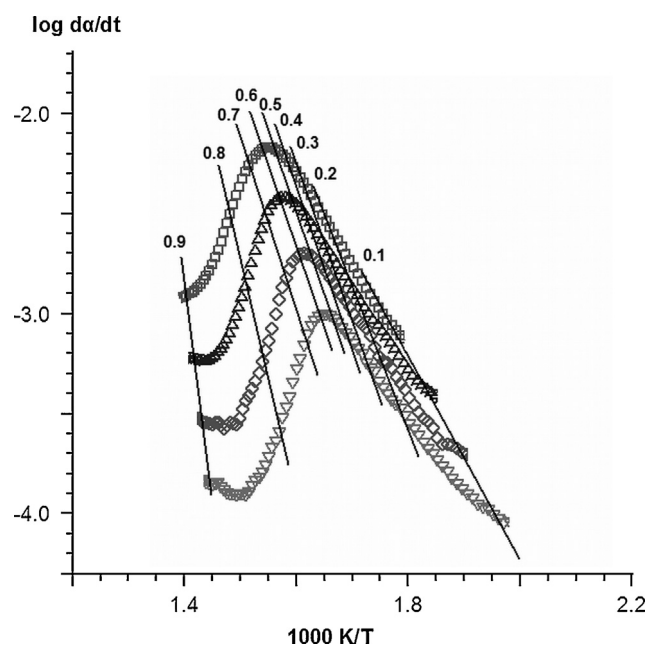


Fig. 2. Plot of $\log d\alpha/dt$ as a function of $1000/T$ according to Friedman method for P5.

Table 2

The kinetic parameter values of P5 calculated by Friedman method and Flynn–Wall–Ozawa method.

α	Kinetic parameters			
	Friedman		Flynn–Wall–Ozawa	
	$\log A$ (s^{-1})	E ($kJ mol^{-1}$)	$\log A$ (s^{-1})	E ($kJ mol^{-1}$)
0.1	5.97	97	4.75	80
0.2	9.42	137	8.39	122
0.3	10.50	151	9.88	141
0.4	10.86	156	10.62	150
0.5	10.77	156	10.97	155
0.6	10.70	155	11.07	157
0.7	11.44	166	11.19	160
0.8	16.03	230	12.95	184
0.9	28.55	415	26.67	391

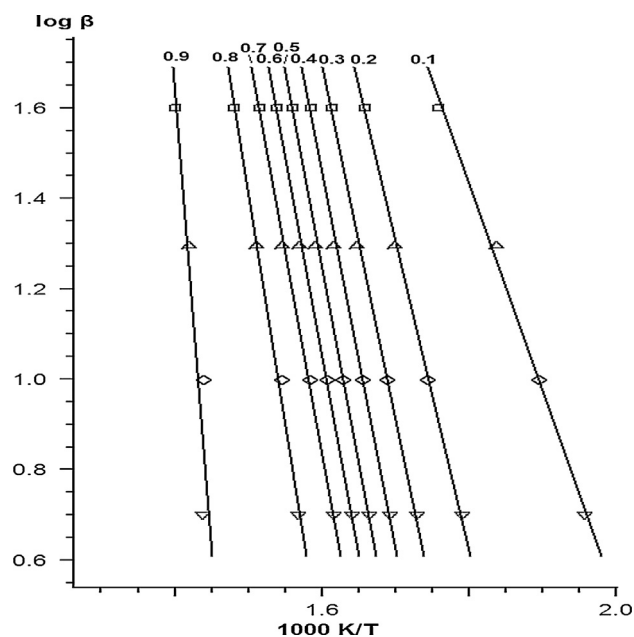


Fig. 3. Plot of $\log \beta$ as a function of $1000/T$ according with Flynn–Wall–Ozawa method for P5.

fact that all analyzed structures, except cellulose, behave similar to P5, a kinetic model of thermal decomposition in four successive stages (Eq. (8)) was proposed. In Eq. (8) sample (A) is transformed into the solid residue (E) through the intermediate stages (B), (C) and (D) and the corresponding gaseous products. Similar, a two stage successive reactions thermal decomposition mechanism was proposed for the pure cellulose and its kinetic thermal degradation parameters values also increased with the conversion degree.



Multivariate non-linear regression method [21] was performed to determine reaction models for the four heating rates and to find the real forms of the conversion functions describing individual decomposition stages of all studied samples. This method, along with the two isoconversional above discussed and used methods, can also be applied for kinetic determinations to some non-degradative thermal processes studied through differential scanning calorimetry [24].

The experimental TGA curves were compared with those simulated by the software, using the isoconversional data. After testing of 13 reaction types [25], the best results were obtained with n

order reaction model (coded Fn), as described by Eq. (9), for pure PVA and the cryogels:

$$f(\alpha) = (1 - \alpha)^n \quad (9)$$

Table 3 lists the codes of the decomposition mechanisms presented in the literature [25] and also the statistical parameters (F_{exp} and F_{crit}) which indicate the fit quality of the calculated curves to the experimental ones for P5.

Multivariate non-linear regression method indicated that the Fn and expanded Prout–Tompkins (Bna) models fit better to former and latter stage of thermal decomposition of pure cellulose with correlation coefficients values of 0.999848 and 0.999738, respectively. The Fn and Bna have both F_{exp} and F_{crit} values of 1.0 and 1.12. The function $f(\alpha)$ for the Bna model is $\alpha^{0.368}(1 - \alpha)^{0.449}$. The E and $\log A$ values for Bna model are 213 kJ mol^{-1} and 16.6 s^{-1} . These values, along with the ones obtained for the Fn model, were found to be situated within the range of the global kinetic parameters obtained by Flynn–Wall–Ozawa and Friedman methods. The Bna model is described as an autocatalytic model [26]. In solid-state kinetics autocatalysis process occurs when nuclei growth promotes continued reactions because of formation of imperfections (i.e., cracks or dislocations) at the reaction interface (i.e., branching). Termination takes place when the reaction starts to spread into the material that has decomposed [27]. The Bna model has been used in a similar study for microgranular cellulose [28] and for nanocomposites polymer non-organic particles [29,30].

The kinetic data obtained by multivariate non-linear regression method are presented in Table 4.

Fig. 4 shows the comparison of experimental data with the calculated data. It was observed that the tabeled correlation coefficients yielded the closest values to unity, thus proving the validity of thermal decomposition models in two and four successive stages, respectively. Furthermore, it can be observed that the kinetic parameters corresponding to each individual decomposition stage for P5 are in the range of global ones determined by the two applied isoconversional methods. The same was observed for the other cryogels and pure comprising polymers.

The first decomposition process of PVA corresponds to water loss (31–217 °C [8]). The value of n close to 2, in the second (217–306 °C [8]), third (306–419 °C [8]) and fourth stage of thermal decomposition (419–513 °C [8]), suggests that the weight loss is related to random main chain scission with shorter polymer fragments formation and intramolecular transfer [12]. The second stage of thermal decomposition was assigned to both partial dehydration and polyene formation [8]. The third stage of thermal decomposition was attributed to polyene decomposition and macroradicals scission. This is considered the main degradation part of the PVA, due to a high degree of mass loss (63% [8]) [31]. The last stage

Table 3
Reactions types and corresponding reactions equations, $de/dt = -A \exp(-E/RT)f(e,p)$; e – concentration of the educt; p – concentration of the solid product, for P5.

Code	$f(e,p)$	Reaction type	Correlation coefficient	F_{crit} (0.95)	F_{exp}
Fn	e^n	n th-Order reaction	0.999855	1.11	1.00
Bna	$e^n \cdot p^a$	expanded Prout–Tompkins equation (na)	0.999534	1.11	1.30
F2	e^2	Second order	0.999254	1.11	1.56
D2	$-1/\ln e$	Two dimensional diffusion	0.998932	1.11	1.58
D1	$0.5/(1 - e)$	One dimensional diffusion	0.998527	1.11	1.60
D4	$1.5 \cdot (e^{-1/3} - 1)$	Three dimensional diffusion (Ginstling–Brounstein type)	0.998211	1.11	1.62
D3	$1.5 \cdot e^{1/3} \cdot (e^{-1/3} - 1)$	Three dimensional diffusion (Jander's type)	0.997556	1.11	1.75
F1	e	First order	0.997111	1.11	1.84
R3	$3 \cdot e^{2/3}$	Three-dimensional phase boundary reaction	0.996786	1.11	1.95
A2	$2 \cdot e \cdot (-\ln(e))^{1/2}$	Two dimensional nucleation	0.996699	1.11	1.98
R2	$2 \cdot e^{1/2}$	Two dimensional phase boundary reaction	0.996788	1.11	1.99
A3	$3 \cdot e \cdot (-\ln(e))^{2/3}$	Three dimensional nucleation	0.996252	1.11	2.03
An	$n \cdot e \cdot (-\ln(e))^{(n-1)/n}$	n -Dimensional nucleation/nucleus growth (Avrami/Erofeev)	0.968765	1.11	13.5

Table 4

Kinetic parameters of the thermal decomposition stages of the cryogels and pure comprising polymers.

Sample	Decomposition stage	Kinetic parameters	Statistical data		
			Correlation coefficient	F_{crit} (0.95)	F_{exp}
PVA	I	$\log A$ (s^{-1}) = 9.00 E ($kJ mol^{-1}$) = 86 n = 2.97	0.999866	1.12	1.00
	II	$\log A$ (s^{-1}) = 5.25 E ($kJ mol^{-1}$) = 85.22 n = 1.95			
	III	$\log A$ (s^{-1}) = 15.58 E ($kJ mol^{-1}$) = 219 n = 1.68			
	IV	$\log A$ (s^{-1}) = 21.26 E ($kJ mol^{-1}$) = 317 n = 2.33			
P1	I	$\log A$ (s^{-1}) = 4.069 E ($kJ mol^{-1}$) = 48 n = 2.68	0.999578	1.12	1.00
	II	$\log A$ (s^{-1}) = 5.706 E ($kJ mol^{-1}$) = 83 n = 2.99			
	III	$\log A$ (s^{-1}) = 13.84 E ($kJ mol^{-1}$) = 185 n = 2.99			
	IV	$\log A$ (s^{-1}) = 24.286 E ($kJ mol^{-1}$) = 309 n = 2.99			
P3	I	$\log A$ (s^{-1}) = 6.839 E ($kJ mol^{-1}$) = 64 n = 2.99	0.999669	1.12	1.00
	II	$\log A$ (s^{-1}) = 5.822 E ($kJ mol^{-1}$) = 88 n = 2.99			
	III	$\log A$ (s^{-1}) = 13.77 E ($kJ mol^{-1}$) = 183 n = 0.8			
	IV	$\log A$ (s^{-1}) = 21.1381 E ($kJ mol^{-1}$) = 274 n = 2.99			
P5	I	$\log A$ (s^{-1}) = 4.9 E ($kJ mol^{-1}$) = 102 n = 2.7	0.999855	1.11	1.00
	II	$\log A$ (s^{-1}) = 5.47 E ($kJ mol^{-1}$) = 82 n = 0.83			
	III	$\log A$ (s^{-1}) = 12.02 E ($kJ mol^{-1}$) = 165 n = 2.99			
	IV	$\log A$ (s^{-1}) = 25 E ($kJ mol^{-1}$) = 377 n = 2.99			
Cel	I	$\log A$ (s^{-1}) = 5.30 E ($kJ mol^{-1}$) = 42 n = 3	0.999848	1.12	1.00
	II	$\log A$ (s^{-1}) = 16.6 E ($kJ mol^{-1}$) = 213 n = 1.7	0.999738		

of thermal decomposition is characterized by complex advanced degradation of the polymer chains and by random scission reactions. The first stage of mass loss from cellulose corresponded to water loss (30–124 °C [8]), whilst the second (124–470 °C [8]) was attributed to main chain scissions leading to the formation of levoglucosan followed by yields of volatile products and char [32]. Macroradicals formed during this stage may further catalyze the thermal decomposition process. At least 19 volatile compounds were found and reported for cellulose pyrolysis [33].

3.3. FTIR analysis of the evolved gases

Fig. 5 shows the tridimensional FTIR spectra of the evolved gaseous products during the thermal decomposition process. As an exemplification, all FTIR and MS spectra were discussed for structure P5, due to the other cryogels similar thermal behavior.

It can be observed from Fig. 5 that the cryogels initially lose physically absorbed water and air. The region 4000–3000 cm^{-1} and 1350–2100 cm^{-1} were attributed to loss of physically absorbed

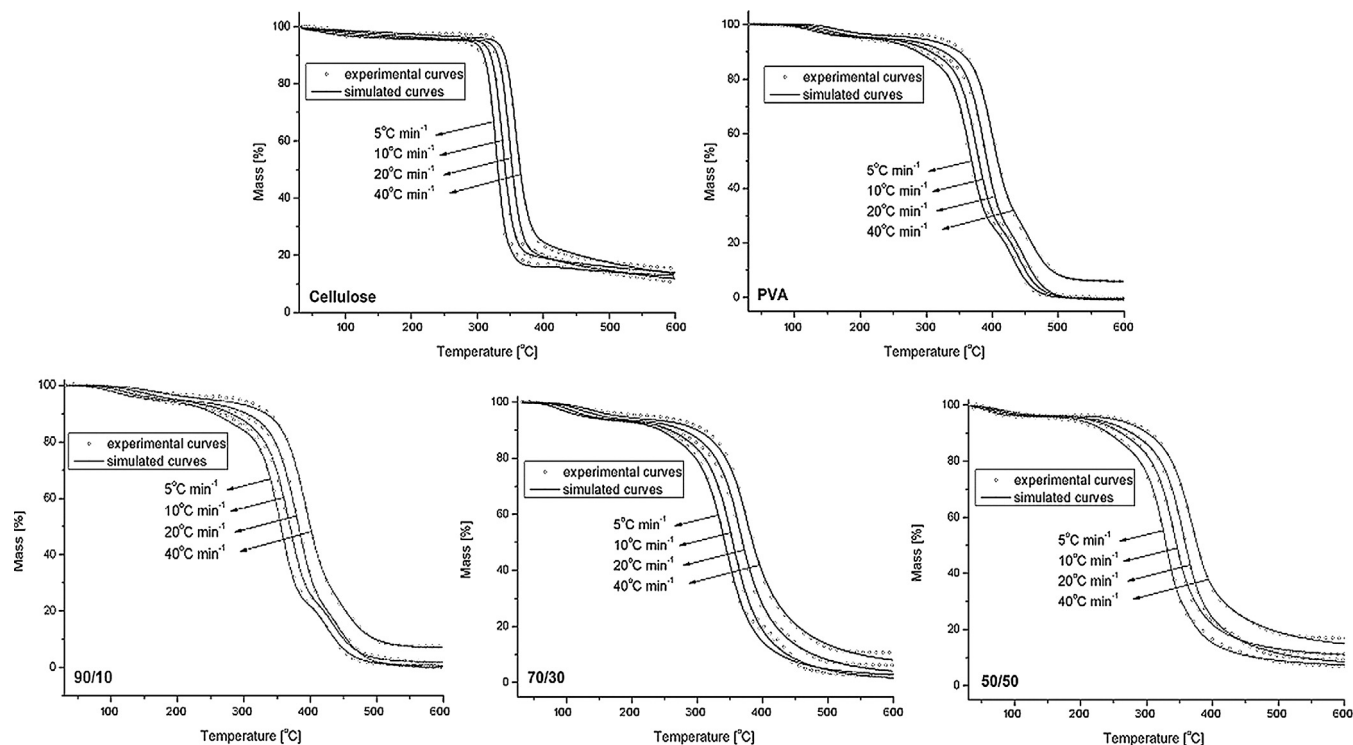


Fig. 4. Comparison of experimental TGA curves with the ones calculated from kinetic data.

water traces [10]. The peak from 2362 cm^{-1} coupled with the signals ranging from 1350 to 2100 cm^{-1} correspond to carbon dioxide traces loss from the physically absorbed air. Fig. 5 shows that the signals intensity corresponding to water and to carbon dioxide continuously increases throughout the whole temperature decomposition process. The signal at 1120 cm^{-1} and the region between 3000 and 3600 cm^{-1} with a peak at 3240 cm^{-1} could correspond to C–OH and O–H stretching vibrations from alcohols [34]. The peak signals at 2181 cm^{-1} and 2114 cm^{-1} correspond to CO evolution [35]. The region 1250 – 2000 cm^{-1} may be attributed to a complex gaseous mixture containing also C=O and C=C stretching vibrations from carbonyl and olefin products. In the thermal decomposition stage during which the highest mass loss occurred, amongst the gaseous mixtures continuously evolved from the previous thermal decomposition stages, there also appears a broad region ranging

between 2800 and 3000 cm^{-1} with a peak at 2937 cm^{-1} corresponding to C–H stretching vibration from CH_3 , CH_2 and CH groups. These peaks become individualized in the last stage of thermal decomposition. New compounds containing carbonyl groups appeared in last stage of thermal decomposition at 1768 , 1749 , 1734 and 1716 cm^{-1} .

3.4. MS analysis of the evolved gases

FTIR spectra and NIST Mass Spectral Database were used for the interpretations of mass spectra. Although the FTIR–MS analysis of the products generated during the thermal degradation of cryogel P5 revealed a complex volatile mixture, only the presence of the most abundant species were taken into account.

The MS analyses confirm the presence of water and air traces in the gaseous mixture. The m/z values of 44, 28, 16 and 12 were attributed to carbon dioxide from air. Also m/z values of 28 and 14 are specific to nitrogen and m/z values of 16 and 32 to oxygen in desorbed air. Water traces were identified by the presence of m/z values of 16, 17 and 18. The loss of absorbed air and water traces is further confirmed by around 2% mass loss in the first stage of gases evolution. The second stage of thermal decomposition also exhibits the all above mentioned gases, except that carbon dioxide is released from the structure and not from the desorbed air. Methanol traces were also identified by m/z values of 31, 32, 29, 28 and 15. The signals at 44, 43, 29 and 15 can be attributed to acetaldehyde resulted from PVA main chain decomposition. Also m/z values of 28 and 12 can correspond to carbon monoxide from cellulose structure decomposition. Ethylene could also be identified in the gaseous mixture by the m/z values of 28, 27 and 26 [36]. The presence of new gases evolution in the second stage of thermal decomposition is confirmed by a higher mass loss of around 6% in comparison with the first stage. The third stage of thermal decomposition exhibits a major mass loss of around 70% due to the presence of the continuously evolved gases from the previous stages and evolution of new compounds. The m/z signals values

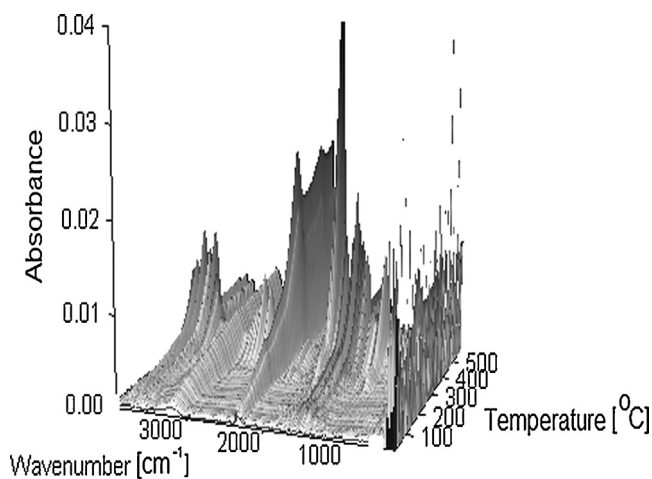


Fig. 5. FTIR spectra of evolved gases during the thermal degradation of P5 recorded as a function of temperature.

raging between 44 and 38 correspond to the formation of ethylene oxide and an increase in acetaldehyde concentration. The CH₃, CH₂ and CH groups identified in the correspondent FTIR spectrum may originate from these structures. The last stage of thermal decomposition is characterized by a massive decrease in mass loss due to the ending of ethylene oxide evolution. The *m/z* signal values at 30, 29 and 28 may correspond to formaldehyde formation.

4. Conclusions

Non-isothermal decomposition kinetic studies of some PVA and cellulose based cryogel materials were conducted by dynamic thermogravimetry, in inert atmosphere and in the temperature range 30–600 °C by recording thermograms at four different heating rates. Global kinetic parameters were determined by applying the isoconversional methods of Friedman and Flynn–Wall–Ozawa. The activation energy values of all samples increased with the conversion degree, thus suggesting a complex mechanism of thermal degradation. Non-linear multivariate regression method was applied to determine the individual kinetic parameters for each stage of thermal decomposition of all studied structures. A Fn model best described the thermogravimetric data for pure PVA and cryogels, whilst the Fn and Bna models better described the two decomposition stages of pure cellulose. During the thermal degradation of cryogels a significant number of gaseous products were identified. The major volatile products evolved during the thermal decomposition were: water, carbon dioxide and olefin and carbonyl structures.

Acknowledgement

Authors would like to thank Dr. Diana Ciolacu of the “Petru Poni” Institute of Macromolecular Chemistry, Iasi, Romania for providing the cellulose.

References

- [1] Y. Nishio, Blends and composites, in: D.R. Gilbert (Ed.), *Cellulosic Polymers, Blends and Composites*, Hanser Publishers, New York, 1994, pp. 95–113.
- [2] M.C. Matias, M.U. de la Oden, C. González-Sánchez, J. Martín-Urreaga, Comparative spectroscopic study of the modification of cellulosic materials with different coupling agents, *J. Appl. Polym. Sci.* 75 (2000) 256–266.
- [3] J. Kuruvilla, T. Sabu, C. Pavithran, Effects of chemical treatment on the tensile properties of short sisal fibre-reinforced polyethylene composites, *Polymer* 37 (1996) 5139–5149.
- [4] B. Liao, Y. Huang, G. Cong, Influence of modified wood fibers on the mechanical properties of wood fiber-reinforced polyethylene, *J. Appl. Polym. Sci.* 66 (1997) 1561–1568.
- [5] H.F. Mark, N.M. Bikales, C.G. Overberger, G. Menges (Eds.), *Encyclopedia of Polymer Science and Technology*, vol. 14, Wiley-Interscience, New York, 1987, p. 45.
- [6] C.C. McCorsley III, J.K. Varga, Process for Making a Precursor of a Solution of Cellulose, U.S. Patent 4 142 913 (1979).
- [7] G. Cazacu, Cellulose, in: C. Vasile, A.P. Chiriac, L.E. Nita (Eds.), *Biodegradable and Biocompatible Polymers*, Tehnopress, Iasi, 2006, pp. 179–186.
- [8] O.M. Paduraru, D. Ciolacu, R.N. Darie, C. Vasile, Synthesis and characterization of polyvinyl alcohol/cellulose cryogels and their testing as carriers for bioactive component, *Mater. Sci. Eng. C* 32 (2012) 2508–2515.
- [9] D. Ciolacu, V.I. Popa, Structural changes of cellulose determined by dissolution in aqueous alkali solution, *Cell. Chem. Technol.* 39 (2005) 179–188.
- [10] C.D. Varganici, A. Durdureanu-Angheluta, D. Rosu, M. Pinteala, B.C. Simionescu, Thermal degradation of magnetite nanoparticles with hydrophilic shell, *J. Anal. Appl. Pyrol.* 96 (2012) 63–68.
- [11] D. Rosu, L. Rosu, M. Brebu, Thermal stability of silver sulfathiazole–epoxy resin network, *J. Anal. Appl. Pyrol.* 92 (2011) 10–18.
- [12] D. Rosu, N. Tudorachi, L. Rosu, Investigations on the thermal stability of a MDI based polyurethane elastomer, *J. Anal. Appl. Pyrol.* 89 (2010) 152–158.
- [13] P. Budrugaec, E. Segal, L.A. Perez-Maqueda, J.M. Criado, The use of IKP method for evaluating the kinetic parameters and the conversion function of the thermal dehydrochlorination of PVC from non-isothermal data, *Polym. Degrad. Stab.* 84 (2004) 311–320.
- [14] M. Villanueva, J.L. Martín-Iglesias, J.A. Rodríguez-Anon, J. Proupin-Castineiras, Thermal study of an epoxy system DGEBA (*n* = 0) MXDA modified with POSS, *J. Therm. Anal. Calorim.* 96 (2009) 575–582.
- [15] J. Opfermann, E. Kaisersberger, An advantageous variant of the Ozawa–Flynn–Wall analysis, *Thermochim. Acta* 203 (1992) 167–175.
- [16] T. Ozawa, A new method of analysing thermogravimetric data, *Bull. Chem. Soc. Jpn.* 38 (1965) 1881–1886.
- [17] J.H. Flynn, L.A. Wall, A quick, direct method for the determination of activation energy from thermogravimetric data, *J. Polym. Sci. Part B: Polym. Lett.* 4 (1966) 323–328.
- [18] C.D. Doyle, Estimating isothermal life from thermogravimetric data, *J. Appl. Polym. Sci.* 6 (1962) 639–642.
- [19] P. Budrugaec, E. Segal, Some methodological problems concerning nonisothermal kinetic analysis of heterogeneous solid–gas reactions, *Int. J. Chem. Kinet.* 33 (2001) 564–573.
- [20] P. Budrugaec, D. Homentcovschi, E. Segal, Critical analysis of the isoconversional methods for evaluating the activation energy. I. Theoretical background, *J. Therm. Anal. Calorim.* 63 (2001) 457–463.
- [21] J. Opfermann, Kinetic analysis using multivariate non-linear regression, *J. Therm. Anal. Calorim.* 60 (2000) 641–658.
- [22] M.G. Grønli, G. Várhegy, C. Di Blasi, Thermogravimetric analysis and devolatilization kinetics of wood, *Ind. Eng. Chem. Res.* 41 (17) (2002) 4201–4208.
- [23] M. Amutio, G. Lopez, R. Aguado, M. Artetxe, J. Bilbao, M. Olazar, Kinetic study of lignocellulosic biomass oxidative pyrolysis, *Fuel* 95 (2012) 305–311.
- [24] C.D. Varganici, O. Ursache, C. Gaina, V. Gaina, B.C. Simionescu, Studies on new hybrid materials prepared by both Diels–Alder and Michael addition reactions, *J. Therm. Anal. Calorim.* 111 (2) (2013) 1561–1570.
- [25] A.K. Galwey, M.E. Brown, Kinetic background to thermal analysis and calorimetry, in: M.E. Brown (Ed.), *Handbook of Thermal Analysis and Calorimetry*, Elsevier Science, Amsterdam, 1998, pp. 179–181.
- [26] A. Khawam, D.R. Flangan, Solid-state kinetic models: basics and mathematical fundamentals, *J. Phys. Chem. B* 110 (2006) 17315–17328.
- [27] P.W.M. Jacobs, Formation and growth of nuclei and the growth of interfaces in the chemical decomposition of solids, *J. Phys. Chem. B* 101 (1997) 10086–10093.
- [28] P. Capart, L. Khezami, A.K. Burnham, Assessment of various kinetic models for the pyrolysis of a microgranular cellulose, *Thermochim. Acta* 417 (2004) 79–89.
- [29] S.M. Lomakin, L.A. Novokshonova, P.N. Brevnov, A.N. Shchegolinkin, Thermal properties of polyethylene/montmorillonite nanocomposites, prepared by intercalative polymerization, *J. Mater. Sci.* 43 (2008) 1340–1353.
- [30] S.M. Lomakin, I.L. Dubnikova, S.M. Berezina, G.E. Zaikov, Kinetic study of polypropylene nanocomposite thermo-oxidative degradation, *Polym. Int.* 54 (2005) 999–1006.
- [31] P. Budrugaec, Kinetics of the complex process of thermo-oxidative degradation of poly(vinyl alcohol), *J. Therm. Anal. Calorim.* 92 (2008) 291–296.
- [32] C. Beyler, M. Hirschler, in: P. DiNenno (Ed.), *SFPE Handbook of Fire and Protection Engineering*, Quincy, Massachusetts, 2002, pp. 110–131.
- [33] X. Wei, Q. Lu, X. Sui, Z. Wang, Y. Zhang, Characterization of the water-insoluble pyrolytic cellulose from cellulose pyrolysis oil, *J. Anal. Appl. Pyrol.* 97 (2012) 49–54.
- [34] R.M. Silverstein, F.X. Webster, D.J. Kiemle, *Spectrometric Identification of Organic Compounds*, Wiley, New York, 2005, pp. 87.
- [35] Q. Liu, Z. Zhong, S. Wang, Z. Luo, Interactions of biomass components during pyrolysis: a TG-FTIR study, *J. Anal. Appl. Pyrol.* 90 (2011) 213–218.
- [36] Q. Liang, C. Wu, Z. Wu, M. Liu, Y. Deng, Q. Gong, Mass spectra of ethylene in intense laser fields, *Chem. Phys.* 360 (2009) 13–17.